Coherent backscatter radar imaging of equatorial spread F: Intermediate scale-size structures

Fabiano S. Rodrigues – Atmospheric & Space Technology Research Associates - ASTRA, Boulder, CO, USA
Eurico R. de Paula – Instituto Nacional de Pesquisas Espaciais - INPE, São José dos Campos, SP, Brazil
Alison de O. Moraes – Instituto de Aeronáutica e Espaço - IAE, São José dos Campos, SP, Brazil

This paper was prepared for presentation at the Twelfth International Congress of the Brazilian Geophysical Society, held in Rio de Janeiro, Brazil, August 15-18, 2011.

Abstract

F-region observations made by a 30 MHz coherent backscatter radar have been used to investigate the morphology of equatorial spread F. Using interferometric radar imaging, two-dimensional in-beam images of scattering structures responsible for ESF echoes have been constructed. The images allow us to resolve the spatial distribution of the scatterers, and to determine, unambiguously, the occurrence of intermediate (a few tens of km) scale-size structures. Here, focus is given to observations made on the night of December 5, 2005. Strong topside and bottomside scattering layers were detected on this night, and well-resolved in-beam images of the scatterers were successfully obtained. Among the imaging results we highlight the detection of narrow, vertically elongated scattering channels spaced by only a few tens of km in the horizontal direction. Such modulation of ESF structures reinforce previous radar imaging results suggesting a possible role of decakilometric plasma waves in ESF development.

1. Introduction

The Generalized Rayleigh-Taylor (GRT) plasma instability is believed to operate in the bottomside of the equatorial ionospheric F region, and is commonly invoked to explain observations of density irregularities in the nighttime equatorial F region (e.g. Kelley, 1989). For historical reasons, the manifestation of these irregularities in observations made by different types of sensors is referred to simply as Equatorial Spread F (ESF). Observations have shown that electron density irregularities with scale-sizes ranging from a few cm to hundreds of km can be detected during spread F events. Typical ESF events are first observed in post-sunset hours in the bottomside F region at the magnetic equator. In some cases, large-scale (hundreds of km) ionospheric plasma depletions are produced by the GRT instability, develop vertically and reach the topside ionosphere. Large-scale ESF events can cause signal disruption in satellite-based communication and navigation systems (e.g., Kintner et al., 2007). Therefore, a better understanding of ESF, which has a high degree of day-to-day variability, has been the subject of numerous research efforts. Prediction of ESF is currently one of the main challenges in space weather.

Much of what is known about ESF comes from radar observations. In fact, radar observations continue to contribute to both basic and applied studies of ESF. Recent studies, for instance, have attempted to use coherent backscatter radar observations to better understand and improve the description of ionospheric channel during ESF events (e.g. Caton et al., 2009; Costa et al., 2011). Based, mostly, on coherent backscatter radar observations made at Jicamarca the Radio Observatory in Peru, it has been suggested that the nighttime F-region echoing structures seen in Range-Time-Intensity (RTI) maps seem to fall within three major categories of ‘layers’ (Woodman and LaHoz, 1976; Hysell and Burcham, 1998). This classification and the main differences between the different types of layers should be kept in mind when comparing radar observations with measurements made by other instruments and with numerical simulations of ionospheric instabilities (Hysell, 2000; Woodman, 2009).

The first type of echoing layer usually seen in RTI maps is the bottom-type. Bottom-type layers appear as relatively weak echoing regions in the RTI maps, and they seem to occur virtually every night over Jicamarca during ESF season. Bottom-type layers are narrow in altitude (a few tens of km) and their occurrence is confined to bottomside F-region heights. The most striking feature of bottom-type layers, which was determined from interferometric radar observations, is the fact that they tend to move in the westward zonal direction. In some cases, bottom-type layers do not seem to move at all, or they move very slowly in the eastward direction. The second type of F-region echoing layer observed in the RTI maps is called the bottomside layer. Botttomside layers are usually confined to heights around and below the F-region peak. RTI maps show bottomside layers as echoing regions that are broader (in altitude) and more structured than the bottom-type layers. There are times, however, when only interferometric observations can distinguish bottomside layers from bottom-tyepe layers. Despite being observed more frequently than topside layers, the bottomside layer does not seem to receive the same amount of attention that is given to topside events (Hysell, 1998). This is, at least in part, because bottomside layers do not seem to be associated with the same level of low-latitude ionospheric disturbances that accompany topside layers. Finally, the third and most impressive, type of echoing structure is the topside layer, also referred to as radar plume because of its appearance in RTI maps (Woodman and LaHoz, 1976). The topside layer is believed to be a manifestation of the so-called ESF depletions or plasma bubbles commonly observed by satellites and airglow instruments (e.g. McClure et al., 1977; Sobral et al., 1980). Topside structures are well developed vertically and, as the name suggests, reach topside ionospheric heights. Radar plumes can reach over 1,000 km altitude during moderate or high solar flux conditions.

In this article, we present new results of a radar study of ESF irregularity structures. Examples of results are shown for observations made on the night of December 5, 2005. On this night, topside plumes were observed by a 30 MHz coherent backscatter radar deployed and maintained by INPE in the equatorial site of Sao Luis. We employed interferometric radar imaging techniques to study the morphology of the scattering layers producing the observed ESF echoes. The morphology the scattering layers can give us insights on underlying plasma processes. This paper is organized as follows: Section 2 describes the experimental setup used for radar observations of ESF irregularities. Section 3 gives a brief description of the in-beam coherent backscatter radar imaging technique. In Section 4, we present and discuss the results of our analyses.

2. Experimental Setup

In 2001, a 30 MHz coherent backscatter radar was deployed in the equatorial site of São Luís (2.59° S, 44.21° W, -2.35° dip lat) in Brazil to study ionospheric irregularities. This radar, since then, has been using one or two 4-kW peak-power transmitters and coded pulses to observe small-scale (5-meter) non-thermal electron density fluctuations (field-aligned irregularities) occurring in the ionospheric E and F regions. Early observations were made with only two antenna modules arranged side-by-side in the magnetic east-west direction. Both antenna sets were used for transmission and reception. Each antenna module is formed by an array of 4×4 Yagi antennas. With two antenna modules, only conventional and single-baseline interferometric observations were possible. Nevertheless, this system allowed real-time monitoring of different types of scattering structures in the Brazilian longitude sector (de Paula et al., 2004a; de Paula et al., 2004b; Rodrigues et al., 2004).

In order to obtain more information about equatorial plasma processes and the irregularities responsible for the echoes detected by the São Luís radar, two more antenna modules were added to the radar system in 2005. The additional sets would allow the construction of interferometric in-beam radar images of the ionospheric scattering layers. Figure 1 shows a diagram with the disposition of the four antenna modules. The antenna modules are aligned with the magnetic east-west direction. Modules A and B in Figure 1 are the original antenna modules and are used both for transmission and reception. Modules C and D are the new antenna modules and are used for reception only. The set of four independent antenna modules can be used to perform interferometry with 6 non-redundant baselines, with baseline lengths varying from 25 to 150 m (2.5 to 15 times the wavelength of the radar signal). The locations of the modules were chosen to give an approximately uniform distribution of baseline lengths.

F-region observations are generally made using full power (two transmitters) and 28-bit long pulses. The inter-pulse period of the soundings is 1,400 km, and baud length of code is 2.5 km. Sampling starts at 200 km altitude.

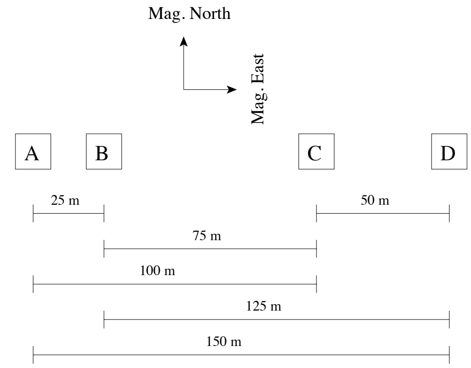

Figure 1: Diagram showing the disposition of the four (A, B, C and D) antenna modules. The modules are aligned in the magnetic east-west direction.

3. Interferometric radar imaging analyses

We use the algorithm described by Hysell (1996) to construct interferometric images of the scattering layers. Here, we give only a brief overview of the technique. We start by expressing the mathematical relationship between the real valued function f that describes the angular distribution of radar scatterers and the complex cross spectrum g computed from signals arriving at two antennas spaced by a distance d:

$$g(kd,\omega) = \int \frac{d\psi}{\sqrt{1-\psi^2}} f(\psi,\omega) A(\psi) e^{ikd\psi} \qquad (1)$$

Here, k is the radar wavenumber, d is the antenna separation in the magnetic zonal direction, ω is the Doppler frequency, ψ is approximately the zenith angle in the magnetic equatorial plane, and $A(\psi)$ is a function representing the antenna pattern in the magnetic east-west direction. Following the notation used in Astronomy, we refer to g as the visibility function and f as the brightness distribution. In radar imaging, we seek $f(\psi,\omega)$, which is the true angular distribution of the Doppler shifted backscattered signals in each radar range gate and for each incoherent integration period. With n antenna modules available, it is possible to obtain estimates of g for $M = n(n-1)/2$ non-redundant baselines. Therefore, g is incompletely sampled, and finding f given a limited, noisy set of measuremets becomes an inversion problem.

To obtain an estimate of $f(\psi,\omega)$, the maximum entropy (MaxEnt) approach for image reconstruction is used. With this technique, one searches for the brightness distribution that maximizes the Shannon (or information) entropy constrained by the measurements and their uncertainties. The discrete version of the Shannon entropy of the brightness distribution is given by:

$$S = -\sum_i f_i \ln(f_i/F) \qquad (2)$$

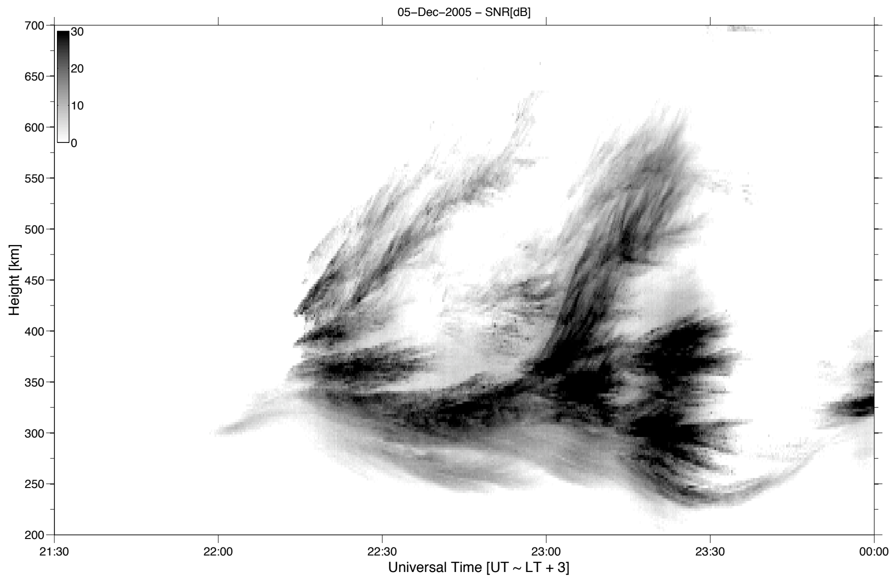

Figure 2: Range-Time-Intensity (RTI) map of F-region observations made by the Sao Luis radar on December 5, 2005.

3.1 In-beam radar images

Two dimensional images are constructed from the one-dimensional spectral brightness distributions $f(\psi,\omega)$ obtained for each range gate. Each spectral estimate is composed of four spectral bins, and each bin is represented by a pure color. Green is used for the zero-frequency component, magenta for the Nyquist frequency component, and red and blue for the red- and blue-shifted components, respectively. For each spectral bin, an image with the respective color associated with the bin is created. The intensity of the color in each pixel is proportional to the signal-to-noise ratio (SNR) of the spectral bin. The four images are added to produce the composite radar images presented in this paper. While pure color images indicate narrow spectral features, color combinations denote broad spectra. White color indicates flat (white) spectra. Conventional Range-Time-Intensity (RTI) maps can be formed by integrating the radar images over all frequencies and zenith angles. The angular coverage of the in-beam radar images is controlled by the radiation patterns of the transmitting and receiving antennas and by the dynamic range of the received echoes. For the São Luís radar, the field-of-view is approximately 16° wide.

4. Results and Discussion

Figure 2 shows the Range-Time-Intensity (RTI) map of the F-region observations made with the Sao Luis radar on the night of December 5, 2005. The RTI map shows that echoes started around 22:00 UT. It also shows that topside plumes were observed before 24:00 UT. Echoes above 600 km altitude were observed suggesting the occurrence of ESF plasma depletions (ionospheric plasma bubbles). Collocated GPS scintillation observations (not show here) confirm the occurrence of plasma bubbles.

Figure 3 shows a sequence of in-beam images generated with observations made by the Sao Luis radar on December 5, 2005 (see Figure 2). Images were generated with a time resolution of about 15 seconds. These images have been combined to produce movies of the scattering structures. These movies show how the scattering structures develop in time and space (zenith angle versus height) within field-of-view (FOV) of the radar beam. Because of the wide FOV of the radar, the development of the structures can be observed during a relatively long time. Here only a few images of the scattering structures are shown (Figure 3). These images, however, illustrate an interesting feature of the scattering layers producing the F-region and topside echoes.

The sequence of images in Figure 3 shows that the echoes observed around 23:08 - 23:18 UT (20:08 - 20:18 LT) were produced by two localized and distinct scattering regions. The first image shows a scattering region formed by a narrow, vertically elongated channel of irregularities with large upward (red-shifted) velocities. The second image shows that this scattering region drifts across the radar beam in the eastward direction, the expected direction of the zonal flow of the background plasma in the F-region during evening hours. The scatterers reach higher altitudes while they drift zonally. A westward tilt of the structure can be clearly observed. The third image shows that a second structure starts to enter the radar FOV coming from West, while the first structure leaves the radar FOV as it moves to East. The zonal separation between these two structures is approximately 40-50 km. The last image shows a better view of the second scattering structure as it enters the radar FOV. Only the upper portion of the first, tilted scattering structure is seen at higher altitudes.

Previous analyses of the Sao Luis radar images indicated the presence of decakilometric plasma waves in the post-

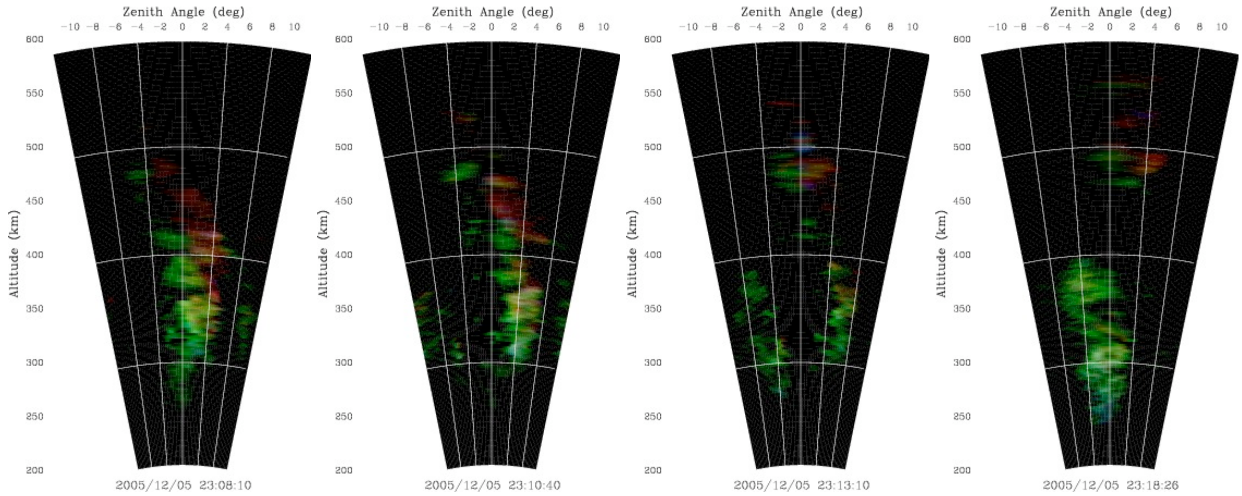

Figure 3: Sequence of in-beam interferometric images produced with observations made by the Sao Luis radar.

sunset equatorial ionosphere (Rodrigues et al., 2008). Similar waves were also observed by the Jicamarca radar in Peru. The origin of these waves has been linked to a collisional shear instability operating the bottomside F-region. More importantly, it has been suggested that these waves could serve as seeding perturbations for the GRT instability. Consequently, it would be expected that ESF structures with similar scale-lengths (a few tens of km) would develop. The interferometric images shown here provide clear evidence of such structures.

Acknowledgements

We would like to thank D. L. Hysell from Cornell University for motivating and clarifying discussions about the radar imaging technique. We also would like to thank the Engineering staff of INPE, particularly Acacio Cunha for operating and maintaining the radar and Lazaro Camargo for managing the radar data. The São Luís radar was partially supported by FAPESP Grants 99/00026-0 and 04/01065-0. This study was only possible thanks to NSF Award AGS 1024849 and AFOSR Grant FA9550-09-C-0205.

References

Caton, R. G., Carrano, C. S., Alcala, C. M., Groves, K. M., Beach, T., and Sponseller, D.: Simulating the effects of scintillation on transionospheric signals with a two-way phase screen constructed from ALTAIR phase derived TEC, Radio Science, 44, 2009.

Costa, E., de Paula, E. R., Rezende, L. F. C., Groves, K. M., Roddy, P. A., Dao, E. V., and Kelley, M. C.: Equatorial scintillation calculations based on coherent scatter radar and C/NOFS data, Radio Sci., 46, 2011.

de Paula, E. R. and Hysell, D. L.: The Sao Luis 30 MHz coherent scatter ionospheric radar: System description and results, J. Geophys. Res., 39, 2004.

de Paula. E. R. et al.: Multi-technique investigations of storm-time ionospheric irregularities over the Sao Luis equatorial station in Brazil, Annales Geophysicae, 22, 2004.

Hysell, D. L.: Radar imaging of equatorial F region irregularities with maximum entropy interferometry, Radio Sci., 31, 1567-1578, 1996.

Hysell, D. L.: Imaging coherent scatter radar studies of bottomside equatorial spread F, Journal of Atmospheric and Solar-Terrestrial Physics, 60, 1,109-1,122, 1998.

Hysell, D. L.: An overview and synthesis of plasma irregularities in equatorial spread F , Journal of Atmospheric and Solar-Terrestrial Physics, 62, 1,037-1,056, 2000.

Kintner, P. M., Ledvina, B. M., and de Paula, E. R.: GPS and ionospheric scintillations, Space Weather, 5, doi:10.1029/2006SW000260, 2007.

McClure, J. P., Hanson, W. B., and Hoffman, J. F.: Plasma bubbles and irregularities in the equatorial ionosphere, J. Geophsys. Res., pp. 2650-2656, 1977.

Rodrigues, F. S. et al.: Equatorial spread F irregularity characteristics over Sao Luis, Brazil, Radio Sci., 39, RS1S31, 2004.

Rodrigues, F. S., D. L. Hysell and E. R. de Paula, Coherent backscatter radar imaging in Brazil: Large-scale waves in the bottomside F-region at the onset of equatorial spread-F, Annales Geophyisicae, 26, 3355-3364, 2008.

Sobral, J. H. A., Abdu, M. A., Zamlutti, C. J., and Batista, I. S.: Association between plasma bubble irregularities and airglow disturbances over Brazilian low latitudes, Geophys. Res. Lett., 7, 980-982, doi:10.1029/GL007i011p00980, 1980.

Woodman, R. F.: Spread-F – an old equatorial aeronomy problem finally resolved?, Ann. Geophys., pp. 1915-1934, 2009.

Woodman, R. F. and LaHoz, C.: Radar observations of F-region equatorial irregularities, J. Geophys. Res., pp. 5447-5466, 1976.